Flow through fish farming sea cages: Comparing computational fluid dynamics simulations with scaled and full-scale experimental data

Heini Winthereig-Rasmussen *, Knud Simonsen, Øystein Patursson

Fiskaaling-Aquaculture Research Station of the Faroes, Við Áir FO-430, Hvalvík, Faroe Islands

ABSTRACT

Computational fluid dynamics (CFD) simulations were performed on the flow through and around full-scale sea cages. The Reynolds average Navier–Stokes equations were solved using a finite volume approach. The realizable $k - \epsilon$ model was used to describe turbulence and porous media to represent the flow resistance effect of the net. Velocity deficit was investigated for a single cage, a row of five cages, and two rows of five cages, corresponding to the salmon farm at Gulin in the Faroe Islands. CFD simulations were compared with field measurement data from this farm. The comparison showed that the flow was overpredicted with up to 50% by the CFD simulations using a net solidity corresponding to the net specifications. A hypothesis is presented for the discrepancy between CFD simulations and field measurements, which includes net deformation and fish behavior. Using different cage layouts, different distances between cage centres, and different net soldities, the effects on flow through and around sea cages were examined and discussed.

© 2016 Elsevier Ltd. All rights reserved.

1. Introduction

The demand for sustainable fish products is ever-increasing and aquaculture has become a main supplier. The production of farmed salmon is showing a stagnating trend in the northern hemisphere (Jones, 2015). One reason, among others, is the lack of coastal space suitable for salmon farming. In the Faroes most of the suitable areas are operational, so in order to expand production the farmers seek more exposed locations or to optimise production on operational farm sites, without leaving a greater biological footprint.

Contributing factors to the stagnation include parasite infections, oxygen deficits, and waste pollution. Some of the more sheltered farm sites experience periods of low oxygen levels. This can induce stress in the fish and lead to deteriorated health and appetite (Oppedal et al., 2011), making the fish more susceptible to severe parasite outbreaks. Low ability to degrade/dissolve waste pollution, i.e. the biological footprint of the fish farming, on sheltered farm sites limits the amount of fish that can be produced (Norði et al., 2011). Being able to perform an accurate simulation of the flow through fish farm sites is a strong tool in overcoming the problems stated above.

Recent field experiments, using boat-mounted acoustic Doppler current profilers (ADCP) and Kriging interpolation, have produced a detailed flow field in the wake of an Atlantic Salmon (Salmo salar) farm site (Winthereig-Rasmussen and Oystein Patursson, 2015). The method has the potential to produce measurements, which can be used as verification of CFD simulations of flow through and around aquaculture farm sites. It has applications in sectors where one seeks full-scale field data of velocity deficit in the wake of bluff bodies, such as the tidal energy and the aquaculture sector. At the same farm site, Klebert et al. (2015) performed measurements of cage deformation and flow velocities inside and outside a net cage over a period of 3 months, overlapping the measurements performed by Winthereig-Rasmussen and Oystein Patursson (2015).

There have been some CFD studies of flow through and around an aquaculture cage of the gravity type (Patursson, 2008; Zhao et al., 2013; Bi et al., 2014). Patursson et al. (2010) introduced a method of substituting the cage nets with a porous media in CFD simulation. They performed experimental measurements on velocity deficit in the wake of a net panel at different angles of attack. The results were transformed into porous media coefficients, which could be implemented in a CFD simulation. Patursson also did measurements on the velocity deficit in the wake of a scale model octagonal aquaculture sea cage of the gravity type (Patursson, 2008). He compared the results with a CFD simulation of flow through the same cage, using porous media as a substitute for the net. Zhao et al. (2013) did a study of up to four cages in a row and looked at velocity reduction through the centre line of the cages. They found only minor flow variation inside the cages by increasing distance between cages. Zhao et al. (2015) recently

---

published an experimental study on flow velocity and mooring loads on scaled net cages arranged in single and double rows with up to eight cages. However all these CFD simulations have been performed on scaled cages, which have been verified with experimental measurements in flumes and tow tanks. Cornejo et al. (2014) performed large Eddie simulations (LES) of a full scale salmon farm in a constant flow and in a semidiurnal tidal current. The model did not include bathymetry data and there were no field measurement data to validate the LES simulation.

In this paper an attempt is made to perform a CFD simulation of the flow through a full-scale commercial salmon farm based on experience gained from previous laboratory experiments and scaled cage simulations (Patursson, 2008; Patursson et al., 2010), and to compare the CFD simulation with field measurements made at the same farm (Winthereig-Rasmussen and Oystein Patursson, 2015; Klebert et al., 2015; Johansson et al., 2014). The focus is on the flow in and around the cages, while potential effects of the relatively flat bottom and the shoreline are not included, but left for further work.

The applied model is described in Section 2, and the location, fish farm, and available data for validation are presented in Section 3. In Section 4 assessment of model parameters and optimisation of the model through mesh sensitivity investigation of flow through a single cage as well as a farm layout are given, and the simulation cases are presented. The results are given in Section 5 and discussed in the following section with emphasis on derived shortcomings when moving numerical simulations from laboratory and scaled cages to a full commercial large salmon farm in production. The paper is concluded in Section 7.

2. Model

CFD simulations were performed using the commercial software ANSYS FLUENT (ANSYS, 2014). Reynolds average Navier–Stokes (RANS) equations were used to describe the flow in the computational domain. The governing equations are the momentum equation

$$\frac{du_i}{dt} = -\frac{1}{\rho}\frac{\partial P}{\partial x_i} + g_i + \frac{\partial}{\partial x_j}\nu_{eff}\left(\frac{\partial u_i}{\partial x_j} + \frac{\partial u_j}{\partial x_i}\right) + \frac{1}{\rho}S_i \tag{1}$$

and the continuity equation

$$\frac{\partial u_i}{\partial x_i} = 0 \tag{2}$$

Einstein notation is applied. u_i is the velocity components, x_i the spatial coordinates, g_i the gravitational force, ρ the density of the fluid and S_i is a source term describing the resistance of the net. ν_{eff} is calculated as μ_{eff}/ρ where $\mu_{eff} = \mu + \mu_t$, P is calculated from the pressure p as $P = p + \frac{2}{3}\rho k$, where $k = u_{rms}^{\prime 2}$ and $u_{rms}^{\prime}$ is the root mean square of the turbulent velocity fluctuations.

The realizable $k - \epsilon$ turbulence model presented by Shih et al. (1995) was chosen in order to close the equation system for turbulence.

The net in the cages is substituted with a porous media in the CFD model, where the resistance parameters are implemented in the source term as follows

$$S_i = -D_{ij}\mu u_j - \frac{1}{2}C_{ij}\rho u_{mag}u_j \tag{3}$$

u_{mag} being the magnitude of the fluid velocity, D_{ij} and C_{ij} being material matrices describing the resistance coefficients in the three local principal axes of the porous media, which if x_1 is the normal to the net plane, have the following form

$$D_{ij} = \begin{bmatrix} D_n & 0 & 0 \\ 0 & D_t & 0 \\ 0 & 0 & D_t \end{bmatrix} \tag{4}$$

and

$$C_{ij} = \begin{bmatrix} C_n & 0 & 0 \\ 0 & C_t & 0 \\ 0 & 0 & C_t \end{bmatrix} \tag{5}$$

In case the local axes of the porous media are not aligned with the global coordinate system, it must be rotated by means of a tensor rotation approach.

A SIMPLEC scheme (van Doormaal and Raithby, 1984) was used for the pressure-velocity coupling, with no skewness correction. A second-order upwind spatial discretisation was used for the momentum equation, turbulent kinetic energy and turbulent dissipation rate, least squares cell based formulation for the gradient and PRESTO for the pressure.

Standard wall function was used on the bottom of the domain and frictionless wall boundary was specified for the vertical sides perpendicular to the inlet/outlet boundary and to the top boundary (Fig. 3). Velocity and turbulence properties k and ϵ were specified at the inlet boundary and were uniform across the entire face.

2.1. Løland's velocity reduction

Løland (1991) derived a theoretical expression for predicting the velocity reduction behind a net panel.

$$\frac{u}{U_0} = 1 - 0.46C_d \tag{6}$$

u being the flow velocity in the wake, U_0 the free flow velocity and C_d the drag coefficient of the net, which is calculated as

$$C_d = 0.04 + (-0.04 + 0.33S + 6.54S^2 - 4.88S^3)\cos\alpha' \tag{7}$$

The solidity (S) of the net is found using

$$S = \frac{2d_{twine}}{\lambda} - \frac{1}{2}\left(\frac{d_{twine}}{\lambda}\right)^2 \tag{8}$$

With d_{twine} as the twine diameter and λ as the length of one mesh bar between twine intersections. α' is the angle of attack (α) of the incoming flow relative to the net and is calculated as $\alpha' = \frac{\pi}{2} - \alpha$.

3. Data

3.1. Fish farm layout

The salmon farm at Gulin is situated in the bay just outside the capital of the Faroe Islands, Trshavn, and during the field measurements consisted of ten sea cages of the gravity type (Fig. 1). Two cages had a circumference of 160 m (cage no. 2 and 10 in Fig. 2), which corresponds to a diameter of about 50 m (D). The rest of the cages had a circumference of 128 m, corresponding to a diameter of about 40 m (d). The cages were positioned in a 2×5 grid formation with 70 m between the cage centres. The short side of the 2×5 cage grid was perpendicular to the flow direction and the long side approximately parallel to the shore (Fig. 2).

The row closest to the shore (cages no. 1, 3, 5, 7 and 9) is referred to as the inner row of cages and the opposite row (cages no. 2, 4, 6, 8 and 10) is referred to as the outer row of cages. The gravity cages stood with vertical net sides of 13 m length and a conical bottom net extending down to a depth of 22 m. The net
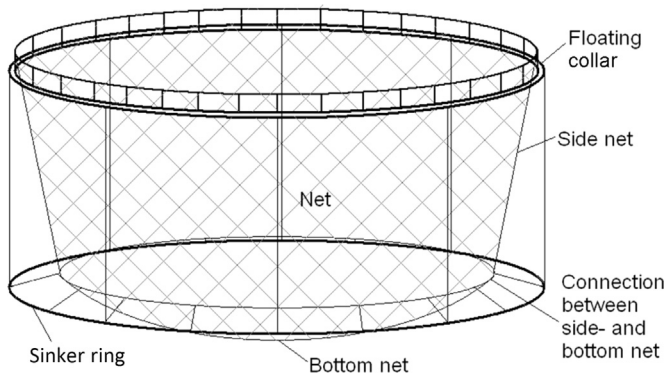
Fig. 1. Schematic overview of a sea cage of the gravity type (Patursson, 2008).

Fig. 3. Boundaries on the CFD model.

properties were a mesh size of 22 mm and a twine thickness of 2.4 mm. Sinker rings were mounted on all cages. Following the numbering in Fig. 2 the sinker ring in cage no. 6 had a linear density of 40 kg/m, cages no. 1, 3, 4, 5, 9 had 50 kg/m, cages no. 7 and 8 had 60 kg/m and lastly cages no. 2 and 10 had 80 kg/m.

3.2. Boat-mounted ADCP data

The 3-dimensional (3-D) flow field in the wake of the sea cages at Gulin was visualised in Winthereig-Rasmussen and Oystein Patursson (2015). The field experiment was conducted during the eastward tidal flow, which produces a flow in the southeast direction at the farm site. A boat-mounted ADCP measured flow velocity while sailing cross-flow transects in the wake of the sea cages. The measured flow velocity transects were normalised with respect to the undisturbed tidal flow velocity and used as a source for a 3-D interpolation to a volume of water encompassing the transects. From this 3-D flow field, cross-profiles at 97.5, 107.5, 122.5 and 137.5 m from the centre of the last down-current cages were extracted. The velocity data from the surface down to the depth of the vertical net sides, 13 m, was subjected to a least-squared average routine. This dataset is a good indicator of the instantaneous flow field present in the wake of a group of sea cages in a 2×5 grid formation. The mean undisturbed tidal flow velocity was 0.57 m/s for the collected transects.

3.3. ADCP and ADV data in and around a net cage

The velocity deficit through and around an operational full-scale salmon sea cage, of the gravity type, is available from Klebert et al. (2015) for the same farm site. They focused the experiment on cage no. 9 (Fig. 2) when the flow was going in the northwest direction at the farm site. Klebert et al. (2015) used bottom-mounted ADCP to measure flow velocity outside the cage and ADV inside the cage. Velocity data were collected through the centre line of the cage at the following distances from the centre of the cage: -32 m, -10 m, 0 m, and 32 m (Fig. 2). ADVs collected data from a depth of 6 m, while near full-depth velocity profiles were available from the ADCP. A time series was chosen when the tidal current had a stable heading and flow velocity. The undisturbed depth mean tidal flow velocity was 0.43 m/s during the field experiment.

3.4. Turbulence parameters

Two sets of turbulence parameters (Table 1) were used in the presented CFD simulations. The medium turbulence parameters are from Patursson (2008), used in CFD simulation of flow through and around a single operational commercial sea cage. The high turbulence parameters are maximum turbulence parameters from field measurements by Thomson et al. (2012), who performed turbulence measurements at potential tidal energy site "Nodule Point" in Puget sound, Washington, USA. This site had a depth of 22 m and sat at a plateau at the periphery of the sound, quite similar to the farm site Gulin. However, the maximum tidal flow velocity at Nodule Point is about twice that of Gulin. With no available data of the turbulence at the farm site, a good estimation
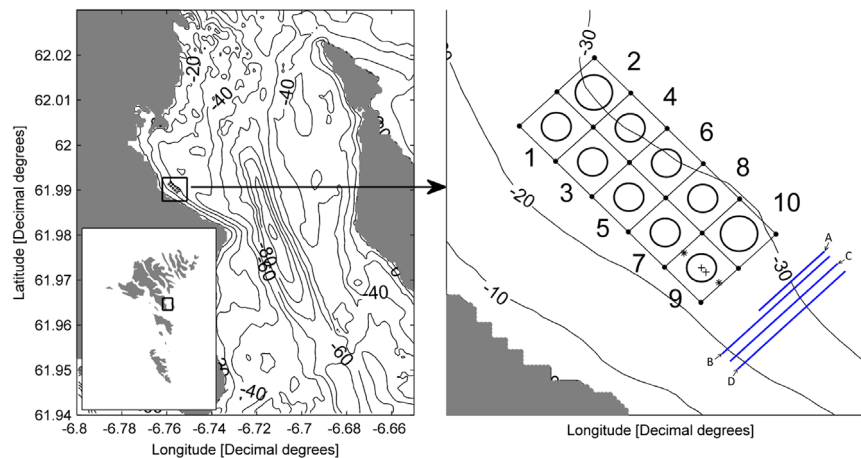

Fig. 2. The bathymetry data of Nólsoyarfjord et al. and the experiment site. Right: The layout of the cages and visualisation of the tidal flow direction. At cage No. 9 the * sign indicates the position of bottom-mounted ADCP and + indicates position of acoustic Doppler velocimeter (ADV) Klebert et al. (2015). Cages no. 2 and 10 are 160 m in circumference and the rest are 128 m. Cross-profiles A–D indicate the position of the velocity cross-profiles in the wake presented in Winthereig-Rasmussen and Oystein Patursson (2015).
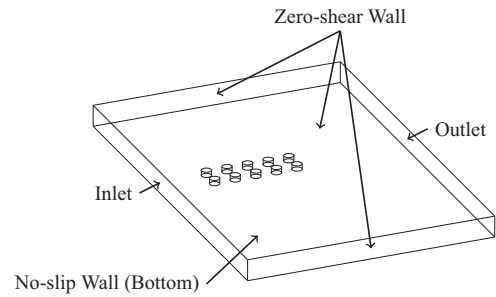
Table 1
Turbulence settings.

Turbulence	k	ϵ
High	3.75×10^{-3}	4.72×10^{-7}
Medium	3.75×10^{-3}	7.55×10^{-6}

Table 2
Porous Media coefficients (Patursson, 2008).

S	$D_n \left(\mathrm{m^{-2}} \right)$	$D_t \left(\mathrm{m^{-2}} \right)$	$C_n \left(\mathrm{m^{-1}} \right)$	$C_t \left(\mathrm{m^{-1}} \right)$
0.20	5173	2637.9	0.5098	0.16984
0.220	10010	3236	0.5952	0.2105
0.317	84537	10590	1.2401	0.65737

is that the turbulence is somewhere in-between these two sets of turbulence settings.

3.5. Porous media coefficients

In this investigation three different net solidities were used in the CFD simulations of the flow through and around sea cages. Patursson (2008) found porous media coefficients for a net solidity of S = 0.20. He used that along with results of S = 0.13, S = 0.243 and S = 0.317 from Rudi et al. (1988) to predict the porous media coefficients of S = 0.22 by means of interpolation. The porous media coefficients for the three solidities are presented in Table 2.

4. Method

The method, which is used for simulating flow through a fish cage, is the porous media model proposed by Patursson (2008), Patursson et al. (2010). As it is too computationally heavy to include all the details of the nets in the fish cage, Patursson et al. (2010) proposed a method where the net is replaced by a porous media, which has the same flow resistance as the net. The porous media coefficients for representing the net were found by performing tow tank experiments of net panels at different angles of attack (Patursson et al., 2010). Patursson et al. then used the method to model flow through a single full scale 30 m in diameter fish cage of the gravity type and compared it with field measurements. Generally there was good correlation between experimental and CFD results inside the cage, but the flow seemed to be underpredicted by the CFD simulation in the wake of the cage. Given the method's computational robustness and overall good correlation with experimental measurements, it was chosen to be applied to the CFD simulation of an entire operational full scale salmon farm consisting of gravity type cages.

Cage deformation simulation of cage no. 9 at a flow velocity of 0.5 m/s (Klebert et al., 2015) showed an about 15% increase in net solidity. This assessment was done by finding the angle of the side net between the undeformed and deformed sea cage. The net does not deform linearly through depth, therefore the angle of each net segment in the simulation is calculated separately and then a mean solidity is found on that basis. Rudi et al. (1988) performed laboratory experiments on net panels of different solidities and found there to be about 10% difference in C_d between nets of solidity S = 0.184 and S = 0.243, which is more than a 30% difference in solidity. A 15% increase in solidity due to deformation would therefore only have a slight additional effect on the C_d of the cages. The bottom beneath the salmon farm is relatively flat and has an constant slope. Due to the complexity involved in modelling the deformation and bathymetry and the fact that this is an initial

attempt to model a full-scale operational fish farm, the deformation and bathymetry is excluded from the CFD model. This decision is evaluated in Section 6.

4.1. Mesh sensitivity study

Patursson (2008) investigated the effect of using three thicknesses 5, 10 and 30 cm of the net substituted porous media and found little difference in the results. In a model of an entire farm the use of an even thicker porous media would reduce the total number of cells needed in the model, thereby reducing the computational cost of running the simulation. Therefore, 2-Dimensional CFD simulations were conducted of a rectangular porous media with a length of 40 m and with two different thicknesses, 30 and 50 cm. The rectangular porous media represent a model of the flat bottom net of a gravity type fish cage, i.e diameter of about 40 m.

The CFD simulations were conducted with an inlet velocity of 1 m/s and turbulence settings of $k = 3.75 \times 10^{-5} \, \mathrm{m^2 \, s^{-2}}$ and $\epsilon = 2.5 \times 10^{-7} \, \mathrm{m^2 \, s^{-3}}$, which were the same inlet settings used by Patursson (2008). The maximum error between the two thicknesses was 2.6%. This is an acceptable error considering the experimental dataset used for comparison with the CFD simulation has an error in the region of about 5% (Winthereig-Rasmussen and Oystein Patursson, 2015). The difference quickly dispersed downstream in the wake of the porous media, so it was decided to use a thickness of 50 cm for the porous media. The study also investigated how many cells were needed through thickness of the porous media in order to converge to a stable solution. The tested number of cells through thickness were: 1, 2, 4 and 8. The result from the study is presented in Fig. 4. It can be seen that the solution converges at four cells through thickness. However two cells is not far off and can be used, if the computational power is limited.

Prior to constructing the mesh for the model of the entire salmon farm, a mesh sensitivity study was performed on a single cage. As the computational domain of the full farm model is $1200 \times 1200 \times 40 \, \mathrm{m}$ (Length × Width × Depth), it is beneficial to optimise the number of cells used in the simulation to keep solution time to a minimum without compromising the quality of the result. The computational domain of the single cage model
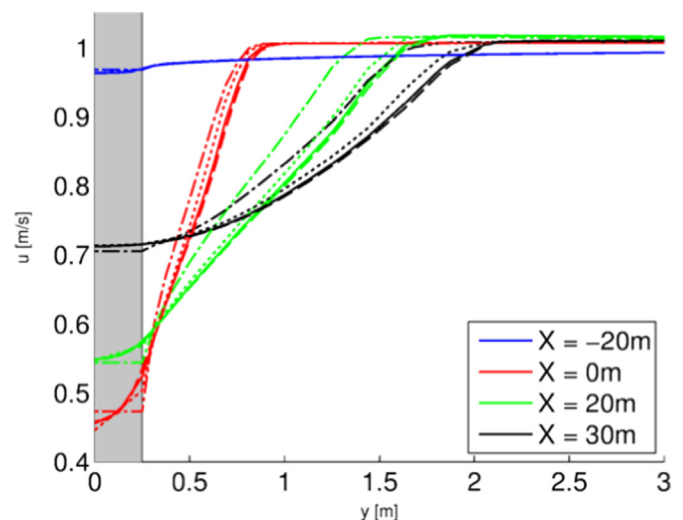

Fig. 4. Comparison between no. of cells through thickness of a porous media. Grey patch illustrates half of the net-replaced porous media. Due to symmetry only half of the model is presented. Solid lines have eight cells, dashed line four cells, dotted line two cells, and the dashdotted line one cell through thickness of a porous media. X-direction is the flow direction with X=0 being the horizontal centre of the net bottom.

was $400 \times 200 \times 40$ m and was conducted in a uniform flow of 0.5 m/s and with medium turbulence parameters (Table 1) and porous media coefficient for S = 0.22 (Table 2). The ANSYS ICEM software was used to construct the mesh and consisted entirely of hexahedral cells.

Having stated the acceptable minimum number of cells in the bottom porous media, focus was shifted to the rest of the computational domain, i.e. the vertical porous media and the water in and around the cage. Three different meshes were tested on the single cage model, a 2.58×10^6 cells mesh with four cells through thickness of the porous media, a 1.21×10^6 cells mesh with two cells through thickness and a 0.55×10^6 cells mesh with four cells through the bottom porous media and one cell through the vertical porous media. As for the vertical porous media, representing the vertical side net wall, there is only a small part that is parallel to the flow. Therefore it does not require as many cells through thickness. Fig. 5 shows that the solution converges with two cells through thickness, but using one cell through thickness only gives a slight deviation of 1% in the vicinity of the point tangent to the flow. Overall there was good correlation between results from the three meshes. So on that basis the mesh with the least number of cells was chosen.

4.2. CFD simulations

Five cases were solved by means of CFD. An overview of the five cases can be viewed in Table. 3. **Case 1** tested three distances of 60 m, 70 m and 80 m between cage centers for two grid layouts, 1×5 and 2×5 cages (Model 1 and 3 in Fig. 6). **Case 2** was a model of the inner row of cages no. 1, 3, 5, 7 and 9 (Model 3 in Fig. 6). The computational domain for the single row of cages model was $1200 \times 600 \times 40$ m, exactly half the width of the full farm model as to preserve pressure distribution over the cages. Two porous media coefficients were used in case 3, S = 0.20 and S = 0.317 (Table 2). **Case 3** used the same model as case 1, but 2 CFD simulations were performed using porous media coefficients equivalent to net solidities of 0.20 and 0.317 (Table 2). **Case 4** was the full farm model consisting of 10 sea cages described in Section

3.1 (Model 1 in Fig. 6). 4 CFD simulations were performed using two inlet velocities, 0.125 and 0.5 m/s, and the two turbulence settings in Table 1. **Case 5** used the single cage model from Section 4.1 (Model 2 in Fig. 6). The CFD model was solved for 14 different inlet velocities ranging from 0.05–1.025 m/s with 0.075 m/s intervals.

5. Results

Case 1 was solved to determine if cage layout formation affects the flow through the cages. Fig. 7A shows a comparison between having 60 m, 70 m and 80 m distances between cage centres in a 2×5 grid formation. It displays the normalised flow velocity through the centre line of the inner row of cages. The minimum normalised velocity through the centre line of a 80×80 m grid with a net solidity of $S=0.22$ was 0.351, whereas it was 0.343 and 0.336 for the 70×70 m and 60×60 m cage grid, respectively. The location of the minimum velocity was just in front of the last cage for 80×80 m and 70×70 m, whereas for 60×60 m it was located in the wake of the last cage. In Fig. 7B the velocity profiles through the centreline of a single row of cages is subtracted from the same velocity profile through the inner row of cages for a 2×5 grid of cages, with respect to their individual distance between cage centres. The largest velocity difference was found in the centre cage (cage no. 5 in Fig. 2) for all distances between cage centres. 60×60 m grid had the largest difference of 0.022, followed by 70×70 m grid with 0.019 and lastly 80×80 m grid with 0.017. All the largest differences where located in the middle cage (cage no. 5 Fig. 2).

The results from case 2 and 3 are presented in Fig. 8. The minimum normalised velocity for one and two rows of cages with S = 0.20 was 0.377 and 0.391, respectively, and located in the wake of the cages. For S = 0.317 the minimum normalised velocities for one and two rows were 0.135 and 0.140, respectively, and located behind the middle cage (cage no. 5 in Fig. 2). The largest difference of 0.034 between the normalised velocity profile for a single and double row of cages was for S = 0.317 and was located in the
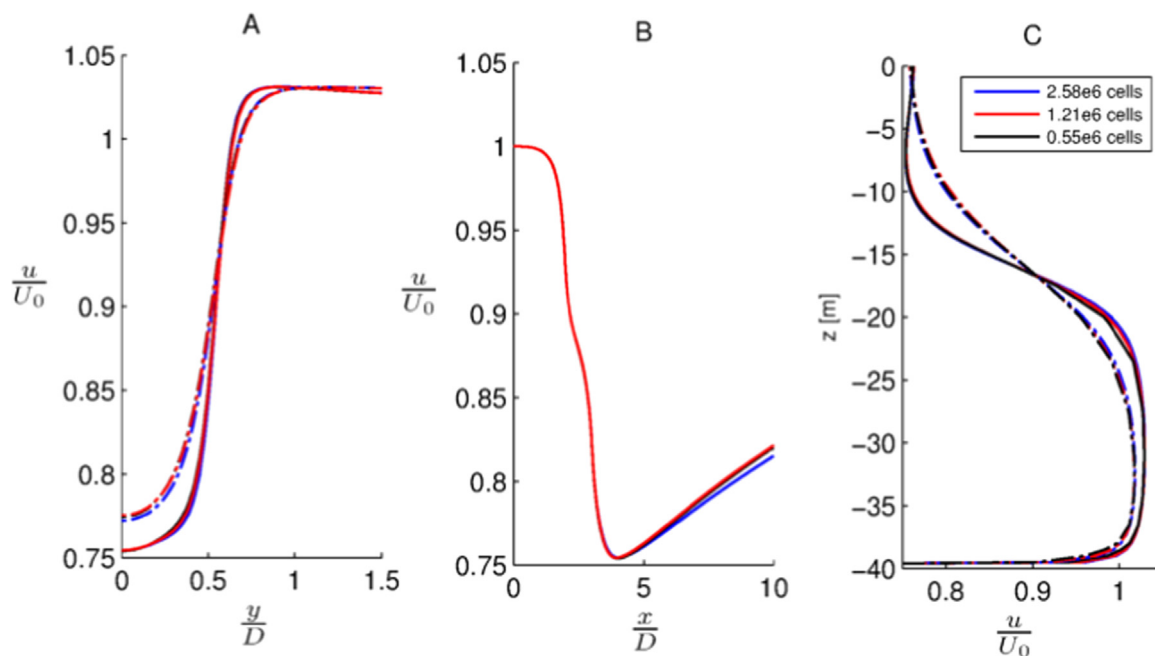

Fig. 5. Chart A: cross-section perpendicular to the flow at a depth of 6 m, solid-line is at $1 \times$ d distances behind the cage and dash-dotted at $3 \times$ d. Chart B: cross-section in the flow direction through the centre line of the wake at depth 6 m. Chart C: cross-section through depth in the centre line of the wake, solid-line is at $1 \times$ d distances behind the cage and dash-dotted at $3 \times$ d.

Table 3
Overview of the five cases that were simulated using CFD.

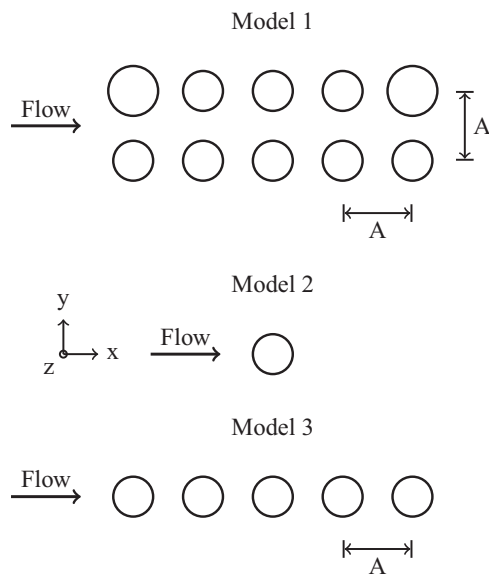| Case	Model (Fig. 6)	A (m) (Fig. 6)	Domain	Mesh size	Inlet velocity (m/s)	Solidity	Turbulence (Table 1)
1	1	60	1200 m × 1200 m × 40 m	4.41×10^6	0.5	0.22	High
	3	70	1200 m × 600 m × 40 m	2.39×10^6			
		80					
2	3	70	1200 m × 600 m × 40 m	2.39×10^6	0.5	0.20	High
						0.317	
3	1	70	1200 m × 1200 m × 40 m	4.41×10^6	0.5	0.20	High
						0.317	
4	1	70	1200 m × 1200 m × 40 m	4.41×10^6	0.125	0.22	Medium
					0.5		High
5	2		400 m × 200 m × 40 m	0.55×10^6	0.05–1.025	0.22	Medium

Fig. 6. Cage layout used in the different CFD models. Model 1 is the actual cage layout of the salmon farm. Model 2 is of a single cage. Model 3 is of the inner row of cages of the salmon farm. A is the distance between cage centres.

Fig. 7. A: Comparison of the flow through the centre line of the inner row of cages in the flow direction at a depth of 6 m for 2 × 5 grid formation with three different distances between cage centres, 60 m, 70 m and 80 m. Experimental results from Zhao et al. (2015) show the normalised velocity inside 2 × 4 cages in a row with a net soldity of $S=0.12$. The x-axis is normalised with the length between cage centers L_g. Grey patches represent the cage positions for the 80×80 m grid formation. Dotted vertical lines represent the cage net position for the 70×70 m grid and dashed vertical lines that of the 60×60 m grid. B: The velocity profiles for 1×5 cages are subtracted from the velocity profile for 2×5 to illustrate the difference of having one or two rows of cages.

second cage (cage no. 3 Fig. 2). For S = 0.20 this difference was 0.017 and located in cage no. 7 (Fig. 2).

Normalised velocity u from the CFD simulations of $S = 0.20$ and $S = 0.317$ in case 3 was extracted at four different cross-profile locations at a depth of 6 m. The locations of the cross-profiles were 97.5, 107.5, 122.5 and 137.5 m from the centre of the last cages in the flow direction (cross-profiles A–D in Fig. 2). The length of the cross-profiles at 97.5, 122.5 and 137.5 m, were normalised with respect to the larger cage diameter of 51 m and centre around the centreline through the outer row of cages when the wake from these cages was evaluated. Oppositely the length of the cross-profiles at 107.5, 122.5 and 137.5 m was normalised with respect to the smaller cage diameter of 41 m and centred around the inner row when this was evaluated. In Fig. 9 the field data and results from the CFD cross-profiles are presented. The outer row had minimum normalised velocities of 0.43, 0.46 and 0.48 (high turbulence Table 1) at the three cross-profiles A,C and D, respectively. The inner row had minimum normalised velocities of 0.45, 0.48 and 0.5 at cross-profiles B, C and D, respectively.

Flow velocity profile through the centre line of cage no. 9 (Fig. 2), at a depth of 6 m was extracted from the CFD results of case 3. In addition to this, through depth velocity profile was extracted at a distance of 32 m from the cage centre in front and behind cage no. 9. Comparisons between field measurements at Gulin (Klebert et al., 2015) and CFD results from case 3 are presented in Figs. 10 and 11.
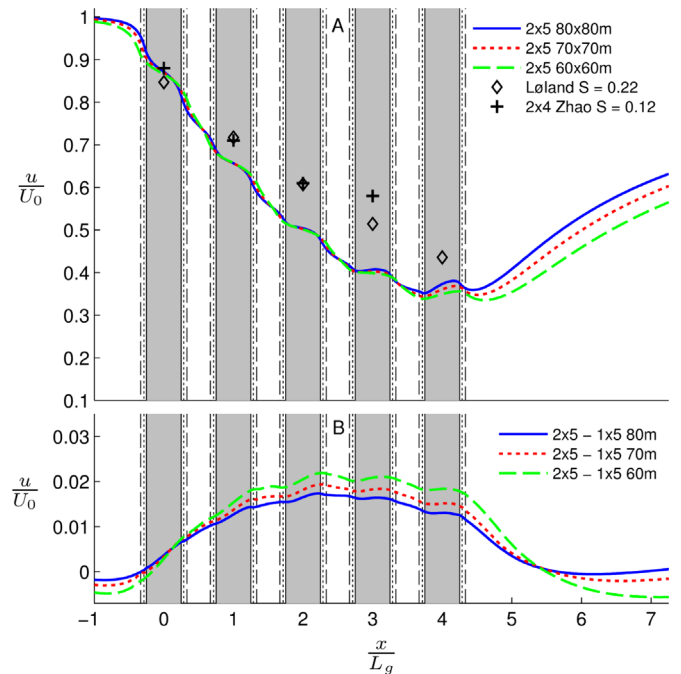
Velocity u in case 4 was normalised with its respective inlet flow velocity, 0.125 m/s and 0.5 m/s. A direct comparison was made between the two results of normalised low and high flow velocity (Fig. 12). For high turbulence settings (Table 1) the minimum normalised velocity was 0.41 for the high inlet velocity and 0.32 for low inlet velocity. For medium turbulence settings the minimum normalised velocities were 0.40 and 0.31, respectively.

In case 5 all the results from the different simulations are normalised with their respective inlet velocity. The normalised velocity profile through the streamwise centre line of the cage at a depth of 6 m was extracted (Fig. 13). The maximum relative difference $\epsilon_{0.5}$ between the velocity profile for an inlet velocity of 0.5 m/s and all the other inlet velocities in case 5, are presented in Table 4. The inlet velocity range of 0.35–1.025 m/s is within a 1% difference.
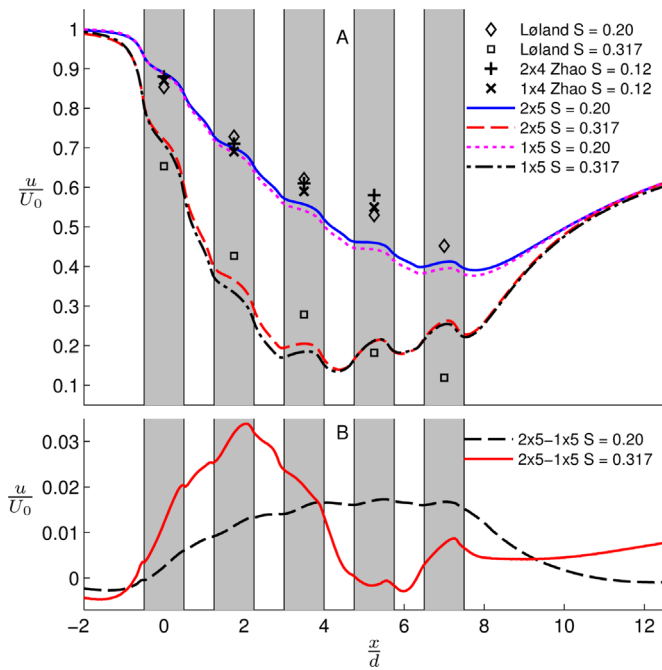
Fig. 8. A: Comparison of the flow through the centre line of the cages in the flow direction at a depth of 6 m for one and two rows of cages in a 70×70 m grid formation with two different solidities. Experimental results from Zhao et al. (2015) show the normalised velocity inside 1×4 and 2×4 cages in a row with a net soldity of $S = 0.12$. B: The difference between one and two rows of cages for both solidities.

6. Discussion

6.1. Distance between cages and cage layout

It was tested how the flow through the sea cages would be affected by changing the distance of 70 m between the cage
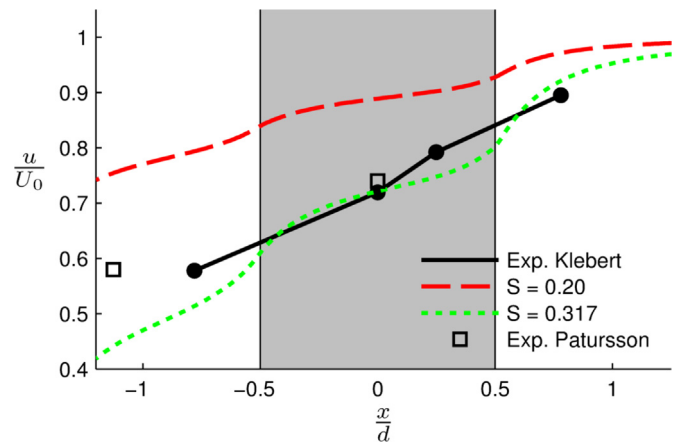

Fig. 10. Comparison between field measurements (Klebert et al., 2015; Patursson, 2008) and CFD case 3 of flow through the centre line of the inner initial cage at a depth of 6 m.

centres by ± 10 m. When comparing the results from case 1 (Fig. 7A), it could be concluded that the flow velocity through the last cages increased by up to 7.3% when comparing 80×80 m grid with 60×60 m. Comparing the actual grid distance of 70×70 m with 80×80 m the flow velocity is increased by 3.6% and when compared to 60×60 m the flow velocity decreased 3.6% through the last cage. The velocity difference is mainly restricted to the last cage as there are minimal differences in the first four cages. When compared to experimental data on flow reduction in scaled cages in a 2×4 grid layout by Zhao et al. (2015), there is seen to be good agreement in the first cage which deviates more downstream. The same correlation is seen when compared to Løland (1991). The solidity on the nets in the study by Zhao et al. was $S = 0.12$, much lower than what was used in case 1, but in shortage of other experimental studies of flow through several cages in a row, this is
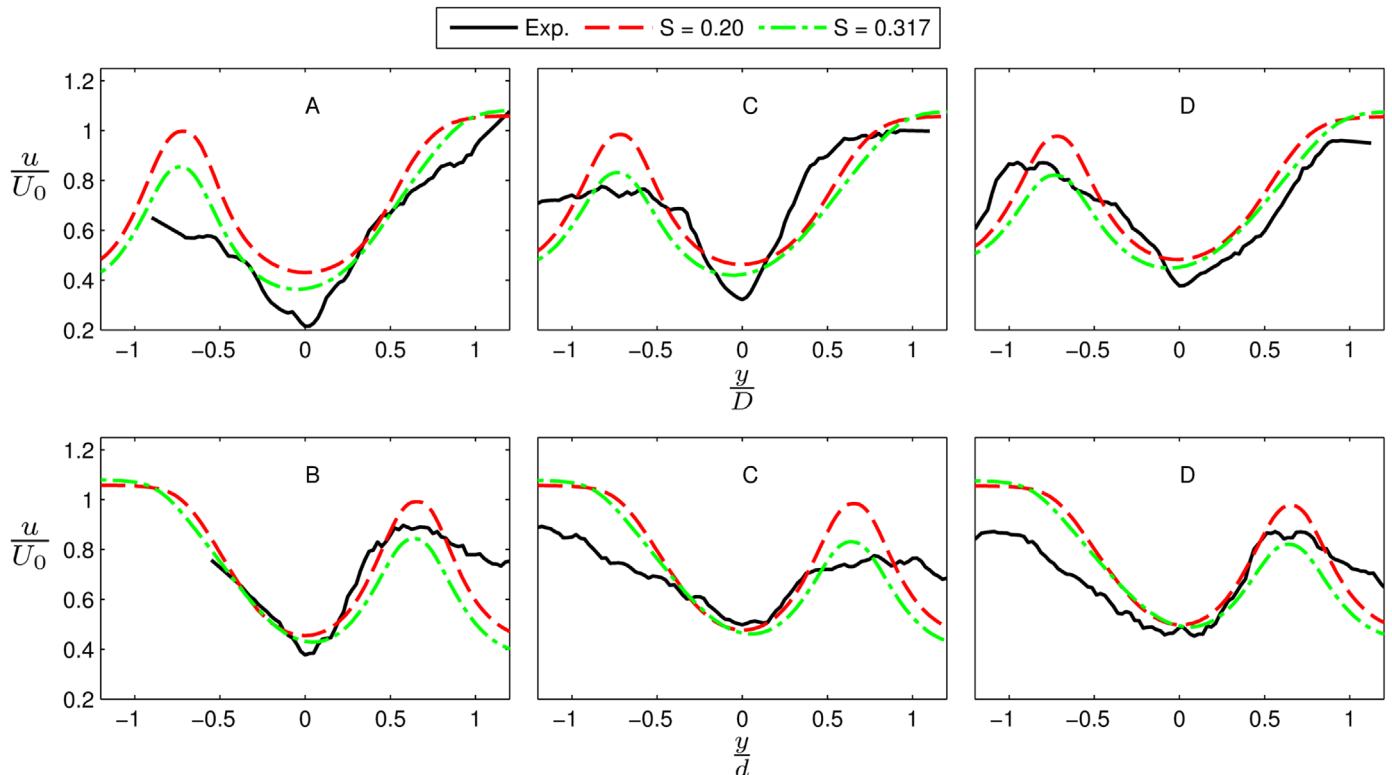

Fig. 9. Comparison of cross-profile flow velocity between field measurements and CFD case 3 with inlet flow velocity of 0.5 m/s. Locations of the cross-profile relative to the cages can be viewed in Fig. 2. The three top plots are relative to the outer row of cages and the three bottom plots are relative to the inner row of cages (Section 3.1).
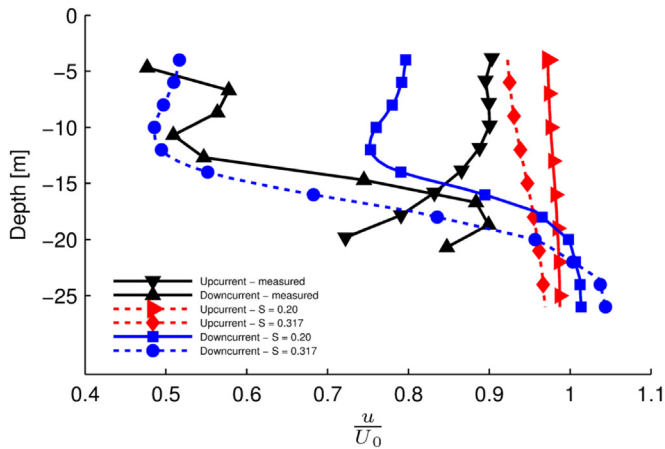
Fig. 11. Comparison between field measurements (Klebert et al., 2015) and CFD case 3 of the through depth flow at both exact position of the two bottom-mounted ADCPs positioned in front and behind the cage.
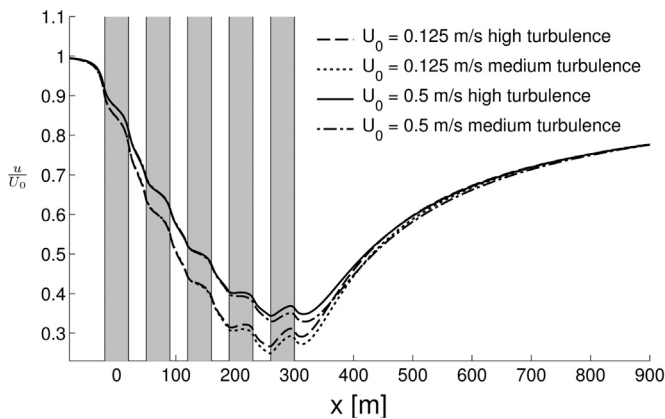

Fig. 12. Case 4. Comparison between normalised low and high speed flow velocity. The velocity profiles were extracted through the centreline of the cages in the inner row of cages. Solid lines represent high turbulence. Dashdotted lines represent medium turbulence.
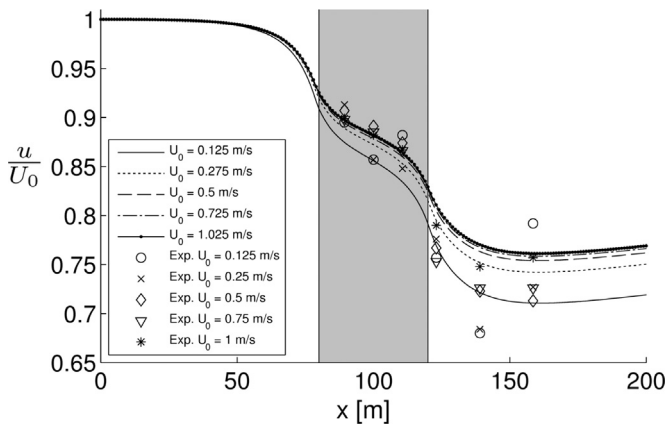

Fig. 13. Case 5. Comparison between normalised velocities from experimental measurements (Patursson, 2008) and CFD simulations in the interval 0.125–1.025 m/s.

the only available data to compare against. In the experiment by Zhao et al. the cages had quite light sinker weights, compared to what is usually used in Faroese farming cages. Therefore there would have been substantial deformation of the upstream cages during the experiments, which would increase the solidity of the nets opposed to the flow direction. This could explain why the difference in velocity reduction in the first cage is so small. Longer

Table 4
The relative difference $\Delta_{0.5}$ between the velocity profile through the centre line of a single cage model (case 5) at a depth of 6 m. $\Delta_{0.5}$ is relative to the inlet velocity $u = 0.5$ m/s. $\frac{u_{min}}{U}$ is the lowest velocity in the wake of the cage.

u (m/s)	$\Delta_{0.5}$(%)	$\frac{u_{min}}{U}$	Re_{twine}
0.05	17.0	0.626	120
0.125	5.8	0.711	300
0.2	2.9	0.732	480
0.275	1.6	0.742	660
0.35	0.8	0.748	840
0.425	0.3	0.752	1020
0.5	0.0	0.754	1200
0.575	0.2	0.756	1380
0.65	0.4	0.757	1560
0.725	0.6	0.758	1740
0.8	0.7	0.759	1920
0.875	0.8	0.760	2100
0.95	0.9	0.761	2280
1.025	1.0	0.761	2460

downstream the deformation would be smaller and therefore the difference in velocity reduction between $S = 0.22$ and $S = 0.12$ is seen to increase.

It was also investigated what the flow velocity difference is between having a 2×5 cage layout compared with a 1×5 cage layout, that is having one or two rows of five cages. The velocity profiles through the centre line of the cages for 1×5 layout with 60×60 m, 70×70 m and 80×80 m grid size were subtracted from the velocity profile through the inner row in the 2×5 layout case with similar grid size (Fig. 7B). This shows that having two rows of five cages increases the flow velocity in the cages by up to 5.5%, 4.7% and 4.1% for 60×60 m, 70×70 m and 80×80 m grid size, respectively, compared with a single row of five cages with identical distances between cage centres. It can be concluded that having two rows of cages will increase flow through the cages, but the increase is small.

In Fig. 8A, the results was compared against experimental results by Zhao et al. (2015) and theoretical results by Løland (1991). Again the solidity from the experimental results is much lower than that of cases 2 and 3, but show good agreement in the first two cages. The reason for the better fit in the second cage in cases 2 and 3 compared to case 1 in Fig. 7, could be that the solidity is lower in cases 2 and 3 compared to case 1. The experimental results by Zhao et al. of 1×4 and 2×4 show the same tendency as seen in the CFD results, which is that the velocity reduction is higher in the single row of cages compared to two rows of cage. The difference is progressing downstream, which is the same in the CFD results. For the case of $S = 0.20$ there is fair agreement between Løland and CFD results, with a little underprediction in the first cage shifting to overprediction in the rest of the cages and a maximum relative difference of 16.1%. In Fig. 8A the minimum flow velocity for $S = 0.317$ is not behind the last cage, as the formula by Løland (1991) shows, but in fact the minimum velocity is found between the middle and penultimate cage downstream. The increase in flow velocity, which is happening after the middle cage, is also not captured by Løland's formula. Løland's formula (Løland, 1991) is applicable under the assumption that the velocity reduction factor is uniform in the entire wake. This is not the case for the flow through circular nets and especially not if the pressure difference over the farm site becomes so high that flow is sucked into the wake from the sides and below the vicinity of the cages, which is a likely explanation for the discrepancies. Zhao et al. (2015) showed similar discrepancies between Løland and scaled experimental results and concluded this to be due to deformation of the nets, which would lead to an increase in solidity. This

conclusion can not be valid here, since the nets are modelled without any deformation.

In analogy with the findings in Section 6.3, it was investigated what the difference is between the velocity profile through the centre line of the inner row when using the higher net solidity $S=0.317$ compared with the net solidity calculated from the net specification $S=0.20$ (Fig. 8) (cases 2 and 3). In addition it was also investigated what the difference is between having one and two rows of five cages, similar to the study in the previous paragraph. The results show that the higher net solidity results in a much larger velocity reduction, which is at its maximum between the middle and penultimate cage (cage no. 5 and 7). This is different for the lower net solidity of $S=0.20$, which has its largest velocity reduction behind the last cage.

When comparing the difference between one and two rows of cages (Fig. 8B), it is seen that the two solidities show different behaviours. For the high solidity case ($S=0.317$) the largest absolute difference is in the second cage (cage no. 3). However, relative to the flow velocity, the largest difference was in the third cage (cage no. 5) and was 13.2%. In the last and penultimate cages there is hardly any difference between one or two rows. In the lower solidity case ($S=0.20$) the difference is seen to steadily increase as the flow progresses through the cages. The largest absolute difference is in the penultimate cage and the largest relative difference of 4.1% is in the last cage. This shows that with increased solidity the flow difference between having one or two rows of cages is more pronounced. At the higher net solidity, water exchange could be optimised by cage layout formation and should be taken into consideration when deploying cages. A larger study should be conducted to investigate this observation over a broader velocity and solidity spectrum. This investigation has the potential to lead to recommendations for fish farmers provided that the flow resistance of the cages including effects from fish and biofouling, is known.

6.2. Inlet velocity dependent reduction

The maximum difference in case 4 was 22–23.1% (Fig. 12), for high and medium turbulence settings (Table 1), respectively. This indicates that the normalised velocity reduction through the porous media is velocity dependent. The difference is present in the direct vicinity of the cages (Fig. 12). In front of and about 1xd downstream in the wake of the cages the difference is negligible. This observation showed that there was a need to examine how the velocity reduction changes within the flow spectrum usually seen in aquaculture of salmons, ie <1 m/s.

Analysing the CFD results from case 5, a maximum difference of 21.6% in normalised velocity reduction is seen in the velocity interval 0.05–1.025 m/s. If compared relative to a inlet velocity of 0.5 m/s, the maximum difference is 17% (Table 4). Patursson (2008)) performed tow tank measurements at different velocities on a octagonal scaled sea cage with a similar solidity of $S=0.22$, as used in the case 5. The comparison between CFD simulation and tow tank results can be seen in Fig. 13. Generally there is a better correlation between experimental and simulation results at higher velocity. For the lower velocity of 0.125 m/s there is a good fit in the center of the cage, but the experimental data is scattered in the wake both above and below the CFD result. The rest of the velocities generally have a good fit inside the cage whereas the CFD simulations underpredict the velocity reduction in the wake. This is similar to what Patursson (2008) concluded. This would indicate that the presented relative differences in Table 4 could in reality be larger.

Comparing case 4 and case 5 for an inlet velocity of 0.125 m/s shows that the velocity reduction difference is accumulating over each sea cage, from 5.8% over a single cage (case 5) to 23.1% over

5 cages (case 4). The largest velocity reduction was between the fourth and fifth cage. It can be concluded that normalised flow field from CFD simulations with an inlet velocity of 0.5 m/s could be used to represent the normalised flow field from the inlet velocity range of 0.35–1.025 m/s within 1% difference over a single cage (Table 4) or about 4% over a row of five sea cages with a net solidity of $S=0.22$.

This knowledge should be kept in mind when conducting field measurements of the velocity deficit behind sea cages. Usually several measurements are needed to produce a time-averaged result. If the averaged velocity data are spread over a large velocity interval involving velocities <0.2 m/s, there is a possibility that the normalised results will not represent the correct velocity reduction. So when conducting such measurements, special care has to be taken to assure that a normalised flow field is in fact representable within the velocity regime in question.

It should be noted that the porous media coefficients were found on the basis of tow tank experiments on net panels at towing speeds between 12.5 and 75 cm/s, so the results from CFD outside of this velocity interval are not absolutely valid and should be thought of as guiding results. To confirm the porous media coefficients outside the velocity interval of 12.5–75 cm/s, the tow tank experiment should be extended to the remaining velocity interval. This falls outside the scope of this paper, as the CFD simulations fall within the valid interval of the porous media coefficients.

6.3. Velocity data comparison over initial cage and in the wake

Due to the distance from the cages to the sidewall boundaries of the computational domain being identical and the bottom being horizontal, the same CFD simulation can be used for evaluating both the eastward and westward tidal current at the farm site. This is useful as the two field measurements (Winthereig-Rasmussen and Oystein Patursson, 2015; Klebert et al., 2015) were done at opposite tidal flow directions. CFD simulation results from case 3 for $S=0.20$, did not correlate well with field measurements conducted by Klebert et al. (2015) (Fig. 10). As seen in Fig. 10 the CFD simulation for $S=0.20$ overpredicted the flow velocity inside the cage by 23.5% and downstream by 37.0%. The difference in front of the cage was 8.7%, indicating that the pressure buildup upstream of the cage is not being represented optimal by the porous media or perhaps there are other factors that are not included in the CFD model, such as bathymetry. In Fig. 11 the measured through-depth flow velocity profile shows a fairly constant flow from the surface down to about 15 m depth. The comparison between measured and simulated data is mainly at a depth of 6 m, so a large effect from the bathymetry is not expected in the top layer. However, there could be interesting effects beneath the cages, which could affect the flow downstream. This needs to be investigated further.

The velocity difference inside and behind the cage is seen to increase exponentially, indicating a too low flow blockage from cages. This would mean that the flow blockage from the cages have been significantly higher during the field measurements, than what can be explained by net specifications alone. There could be three reasons for this: biofouling, net deformation, or flow blockage from the fish inside the cage. The reality is probably a combination of all three. There was no quantitative assessment of the biofouling, but visual inspections were performed, which showed no to very little biofouling. This is also likely, due to the fact that the nets are cleaned regularly at the salmon farm and the time of the field measurements was outside of the peak growth season of biofouling. Therefore the effect of biofouling can be excluded as the main contributor to the increased flow blockage seen between measured and simulated results.

In the comparison between field measurements and CFD simulations (Fig. 9), the results from the CFD simulations are overpredicting the flow velocity. However, there is a clear distinction between the inner and outer row of cages. At the outer row there is a maximum difference of 50% between simulated and measured flow velocity at cross-profile A. The maximum difference in flow velocity at the inner row is 17%. For both wakes the largest difference was found in the cross-profile closest to the cages and decreases with distance downstream in the wake. This indicates that there is some effect that is increasing the flow reduction to a higher degree in the outer row compared with the inner row.

In Section 3.1 it was explained that the heaviest sinker rings are under cage no. 2 and 10 in the outer row, and combined there are more weights in this row. For this reason, there is likely to be less cage deformation in the outer row compared to the inner row, although there is a small current velocity gradient of about 6% across the farm site, decreasing towards the shore. Therefore the net deformation cannot be the sole explanation for the discrepancy between simulated and measured flow velocities.

Cage deformation was excluded from the CFD simulations, as described in Section 4. The additional effect on solidity was determined to be about 15%, which would increase the net solidity to $S = 0.23$. The velocity difference in the center of the initial cage is 2.2%, when comparing CFD results from $S = 0.20$ and $S = 0.22$. The effect from including the net deformation is therefore thought to be in this vicinity, as the deformed net solidity is slightly more than $S = 0.22$. The difference in the downstream cages should be less as these cages do not deform as much, due to the velocity reduction.

Johansson et al. (2014) observed fish behaviour in cage no. 9 (Fig. 2) at the beginning of the field measurements of Klebert et al. (2015). They concluded that three schooling patterns were present depending on the current velocity. At the current velocity present during field measurements conducted by Winthereig-Rasmussen and Oystein Patursson (2015) and Klebert et al. (2015), 0.57 m/s and 0.43 m/s respectively, the salmon were swimming up against the current in a dense group, positioned close to the upstream net side with no forward movement. This fish behaviour is strongly believed to affect the flow through the cage. This hypothesis is supported by the field measurements by Winthereig-Rasmussen, which showed that the largest velocity deficit was behind the outer row, which included the larger sea cages no. 2 and 10 (Figs. 2 and 9). There were approximately 110,000 salmon in each of cages no. 2 and 10 and about 65,000 salmon in each of the other cages. The net deformation should be lower in cages no. 2 and 10 compared to cages no. 1 and 9, as they had the heaviest sinker rings. This makes them more resistant to deformation when subjected to the tidal flow, thereby producing a smaller velocity deficit in the wake compared to cages with lighter sinker rings. This observation indicates strongly that the effect from schooling fish has a substantial impact on the flow; not to be ignored when considering the flow through and around fish farming sea cages. Similar observations, of higher velocity reduction than what can be explained by net specification in stacked net cages, have been made by Johansson et al. (2007), but at lower flow velocity than in this study. Chacon-Torres et al. (1988) also showed that stocked cages of rainbow trout could increase water exchange by their motion in the cage.

Patursson (2008) did flow reduction measurements over a single full-scale fish cage of the gravity type. The cage had clean nets and did not contain any fish during the measurements. The nets had an solidity of $S = 0.15$, but during the measurements the nets were blocked by a high concentration of jellyfish strongly affecting the solidity of the net. While performing CFD simulations to compare the measurements with, Patursson chose the solidity of $S = 0.317$, to represent the net and biofouling. The results from

the velocity reduction measurements by Patursson (2008) and the velocity profile through the cage for $S = 0.317$ can be seen in Fig. 10. The interesting part is that Patursson experienced almost exactly the same deviation between measured and simulated results. That is that the results correlated well in the centre of the cage, whereas the CFD model overpredicted the flow reduction in the wake of the cage. Patursson (2008) concluded that as the jellyfish only blocked the net in front of the cage and not the net in the back of the cage and the solidity must therefore have been too high in the net on the back of the cage and produced a too high flow reduction. That is why the CFD results correlated well in the centre of the cage and not in the wake of the cage. With the salmon behaviour documented by Johansson et al. (2014) in mind, the scenario could very well have been the same for the deviation presented in Fig. 11, where the salmons only affect the flow reduction at the up-current net and not the net in the back of the cage. It could perhaps also be possible to include the fish effect into the porous media as added resistance based on this behaviour. It is seen that the higher solidity of $S = 0.317$ has a much better fit with measurements, as seen in Figs. 10 and 11. Again this is an indication that the salmon inside the cage strongly affect flow reduction through the cage at high currents. It is recommended that the effect from schooling fishes are to be investigated further, especially the effect they have on flow blockage.

Despite the difference in net solidity, CFD results show that the flow velocity in the wake was the same for the two solidity cases ($S = 0.20$ and $S = 0.317$) from around 2xD and outward. This could explain why the velocity difference between measured and simulated results in the cross-profiles are becoming smaller downstream in the wake.

The wakes behind the two rows of cages from the CFD simulations are spaced further apart and are symmetrical around the centre line of the cages compared to measured data by Winthereig-Rasmussen and Oystein Patursson (2015), which showed that the wakes were offset to the left relative to the centre line of the cages. The wake from the inner row of cages was following the curvature of the shoreline (Fig. 2) at a more dominant manner, opposed to the wake from the outer row of cages and thereby ended up having a lesser distance between them than the grid distances, which is what the wakes were in the results from case 3. The discrepancy is likely caused by the shoreline not being included in the CFD simulations. It is unknown if the bathymetry beneath the farm site could have affected the progression of the wake and the flow inside the cages. Future CFD simulations should be performed with shoreline and bathymetry data from Gulin implemented in the CFD model.

It should be emphasised that the results from Winthereig-Rasmussen et al. (2015) do not represent a completely statistical mean flow field, so the direct comparison performed with CFD results has a level of uncertainty. However, due to the interpolation being statistically weighted and the measured data curves in Fig. 9 being averages of the depth 0–10 m, the data are accurate enough for maximum velocity deficit evaluation.

7. Conclusion

A CFD simulation was performed of the flow through and around a commercial salmon farm site consisting of 10 sea cages. The results were compared against two field measurement datasets, which were obtained at the farm site Gulin. There were discrepancies between simulated and measured data. The velocity deficit was higher in the field measurements compared to the CFD simulations. Two likely reasons for these discrepancies were discussed. One was that the nets had an increased net solidity from cages being deformed by the flow. The second was a blocking

effect from the fish inside the cage. It was concluded that the blocking effect from the fish was the larger of these two. No method of including the effect of the fish in CFD simulations is available. On the basis of the findings in this paper it is recommended that relationship between fish behaviour and net solidity at high currents is established. Knowing the exact solidity of an operational cage is crucial in order to correctly simulate the flow through and around a farm site.

The flow reduction between having one or two rows of cages was investigated at different distances between cage centres and for three solidities. It was concluded that having two rows is beneficial from a water exchange point of view, as it consequently shows an increase in flow velocity compared to one row. Changing the distance between cage centres by ± 10 m showed little effect on the flow through the cages, however, there was a tendency for the velocity to increase in the last cage when the distance between cage centres was increased.

Acknowledgements

References

ANSYS ® Academic Research, Help System, FLUENT User guide, release 15.0, ANSYS, Inc.

Bi, C.-W., Zhao, Y.-P., Dong, G.-H., Zheng, Y.-N., Gui, F.-K., 2014. A numerical analysis on the hydrodynamic characteristics of net cages using coupled fluid-structure interaction model. Aquac. Eng. 59, 1–12. http://dx.doi.org/10.1016/j.aquaeng.2014.01.002 〈http://www.sciencedirect.com/science/article/pii/S014486091400003X〉.

Chacon-Torres, A., Ross, L., Beveridge, M., 1988. The effects of fish behaviour on dye dispersion and water exchange in small net cages. Aquaculture 73 (1), 283–293. http://dx.doi.org/10.1016/0044-8486(88)90062-2 〈http://www.sciencedirect.com/science/article/pii/0044848688900622〉.

Cornejo, P., Sepúlveda, H.H., Gutiérrez, M.H., Olivares, G., 2014. Numerical studies on the hydrodynamic effects of a salmon farm in an idealized environment. Aquaculture 430, 195–206. http://dx.doi.org/10.1016/j.aquaculture.2014.04.015 〈http://www.sciencedirect.com/science/article/pii/S0044848614001811〉.

van Doormaal, J.P., Raithby, G.D., 1984. Enhancements of the simple method for predicting incompressible fluid flows. Numer. Heat Transf. Part A: Appl. 7, 147–163. http://dx.doi.org/10.1080/01495728408961817.

Johansson, D., Juell, J.-E., Oppedal, F., Stiansen, J.-E., Ruohonen, K., 2007. The influence of the pycnocline and cage resistance on current flow, oxygen flux and swimming behaviour of atlantic salmon (salmo salar l.) in production cages. Aquaculture 265 (1–4), 271–287. http://dx.doi.org/10.1016/j.aquaculture.2006.12.047 〈http://www.sciencedirect.com/science/article/pii/S0044848606009197〉.

Johansson, D., Laursen, F., Fernö, A., Fosseidengen, J.E., Klebert, P., Stien, L.H., Vågseth, T., Oppedal, F., 2014. The interaction between water currents and salmon swimming behaviour in sea cages. PLoS One 9 (5), e97635. http://dx.doi.org/10.1371/journal.pone.0097635, http://dx.doi.org/10.1371%2Fjournal.pone.0097635.

Jones, M., © fao 2004–2015. cultured aquatic species information programme. salmo salar. 〈http://www.fao.org/fishery/culturedspecies/Salmo_salar/en#tcNA00D6〉.

Klebert, P., Patursson, Ø., Endresen, P.C., Rundtop, P., Birkevold, J., Rasmussen, H.W., 2015. Three-dimensional deformation of a large circular flexible sea cage in high currents: Field experiment and modeling. Ocean Engineering 104, 511–520. http://dx.doi.org/10.1016/j.oceaneng.2015.04.045, URL http://www.sciencedirect.com/science/article/pii/S0029801815001262.

Løland, G., 1991. Current Forces on and Flow Through Fish Farms (Ph.D. thesis). University of Trondheim.

Norði, G., Glud, R.N., Gaard, E., Simonsen, K., 2011. Environmental Impacts of Coastal Fish Farming: Carbon and Nitrogen Budgets for Trout Farming in Kalbaksfjørður (Faroe Islands), vol. 431, pp. 223–241. 〈http://dx.doi.org/10.3354/meps09113〉.

Oppedal, F., Dempster, T., Stien, L.H., 2011. Environmental drivers of atlantic salmon behaviour in sea-cages: a review. Aquaculture 311 (1–4), 1–18. http://dx.doi.org/10.1016/j.aquaculture.2010.11.020 〈http://www.sciencedirect.com/science/article/pii/S0044848610007933〉.

Patursson, Øystein, Swift, M.R., Tsukrov, I., Simonsen, K., Baldwin, K., Fredriksson, D.W., Celikkol, B., 2010. Development of a porous media model with application to flow through and around a net panel. Ocean Eng. 37 (2–3), 314–324. http://dx.doi.org/10.1016/j.oceaneng.2009.10.001 〈http://www.sciencedirect.com/science/article/pii/S0029801809002406〉.

Patursson, Ø., 2008. Flow through and around fish farming nets, Ph.D. dissertation, Ocean Engineering, University of New Hampshire, Durham, NH 03824, USA.

Rudi, H., Løland, G., Furunes, I., 1988. Modellforsøk med nøter. krefter og gjennomstrømning på enkeltpaneler og merdsystem, Tech. Rep. mt51 F88-0215, Marintek, Trondheim, Norway, (In Norwegian).

Shih, T.-H., Liou, W.W., Shabbir, A., Yang, Z., Zhu, J., 1995. A new k-ε eddy viscosity model for high reynolds number turbulent flows. Comput. Fluids 24 (3), 227–238. http://dx.doi.org/10.1016/0045-7930(94)00032-T 〈http://www.sciencedirect.com/science/article/pii/004579309400032T〉.

Thomson, J., Polagye, B., Durgesh, V., Richmond, M., 2012. Measurements of turbulence at two tidal energy sites in puget sound, WA. IEEE J. Ocean. Eng. 37 (3), 363–374. http://dx.doi.org/10.1109/JOE.2012.2191656.

Winthereig-Rasmussen, H., Patursson, Øystein, Simonsen, K., 2015. Visualisation of the wake behind fish farming sea cages. Aquac. Eng. 64 (0), 25–31. http://dx.doi.org/10.1016/j.aquaeng.2014.12.001 〈http://www.sciencedirect.com/science/article/pii/S0144860914001174〉.

Zhao, Y.-P., Bi, C.-W., Chen, C.-P., Li, Y.-C., Dong, G.-H., 2015. Experimental study on flow velocity and mooring loads for multiple net cages in steady current. Aquac. Eng. 67, 24–31. http://dx.doi.org/10.1016/j.aquaeng.2015.05.005 〈http://www.sciencedirect.com/science/article/pii/S014486091500045X〉.

Zhao, Y.-P., Bi, C.-W., Dong, G.-H., Gui, F.-K., Cui, Y., Xu, T.-J., 2013. Numerical simulation of the flow field inside and around gravity cages. Aquac. Eng. 52 (0), 1–13. http://dx.doi.org/10.1016/j.aquaeng.2012.06.001 〈http://www.sciencedirect.com/science/article/pii/S0144860912000593〉.